

Comparison of ^{18}F FDG PET / CT, MRI (DWI + DCE) and MRI + ^{18}F FDG PET/CT in the detection of axillary metastatic lymph nodes in patients with newly diagnosed breast cancer

Hasan Gundogdu¹, Osman Kupik²

¹Department of Radiology, Recep Tayyip Erdoğan University, Faculty of Medicine, Rize, Turkey

²Department of Nuclear Medicine, Sıtkı Koçman University, Faculty of Medicine, Muğla, Turkey

ABSTRACT

Aim: We visually and quantitatively investigated the success of using 2-deoxy-2-[fluorine-18] fluoro-D-glucose integrated with computed tomography (^{18}F -FDG PET/CT) and magnetic resonance imaging (MRI) [Dynamic contrast enhancement (DCE) and diffusion weighted imaging (DWI)] separately and together in detecting axillary lymph node metastasis in patients with newly diagnosed breast cancer.

Methods: One hundred and thirteen patients who underwent ^{18}F FDG PET/CT were evaluated, 102 patients of these patients had also MRI (DEC + DWI). Primary tumour size (Tsize), SUVmax of primary tumour (SUVmaxT), short diameter of largest axillary lymph node on PET/CT (LnDPET/CT), SUVmax of axillary lymph node (SUVmaxLn), metabolic tumour volume of the primary tumour (MTV), short diameter of largest axillary lymph node on MRI (LnDMRI), the presence of fatty hilum absence and apparent diffusion coefficient (ADC) were evaluated.

Results: In visual analysis, sensitivity and specificity values of ^{18}F FDG PET/CT, MRI and MRI+ ^{18}F FDG PET/CT were 78.85, 94% – 72.27%, 96.15 – 83.87%, 98.04%, respectively. In the quantitative evaluation, $\text{ADC} \leq 1.2 \times 10^{-3} \text{ mm}^2/\text{sec}$ (OR = 6.665, $p = 0.001$, 95CI%: 2.181–20.370) and $\text{LnSUVmax} > 2$ (OR = 15.2, $p < 0.001$, 95CI%: 4.587–50.376) were independent predictors in detecting axillary lymph node metastasis.

Conclusion: $\text{LnSUVmax} > 2$ and $\text{ADC} \leq 1.2 \times 10^{-3} \text{ mm}^2/\text{sec}$ can be used as independent predictors of detecting axillary lymph node metastasis in patients with newly diagnosed breast cancer.

Key words: Breast neoplasms, lymphatic metastasis, fluorodeoxyglucose F18, PET / CT, MRI.

✉ Dr. Hasan Gundogdu

Department of Radiology, Recep Tayyip Erdoğan University, Faculty of Medicine, Rize, Turkey

E-mail: hasangundogdu@gmail.com

Received: 2021-02-08 / Revisions: 2021-04-10

Accepted: 2021-04-12 / Published online: 2021-07-01

Introduction

The presence of axillary lymph node metastasis (ALNM) is important for the prognosis of breast cancer and has an impact on treatment management [1]. Sentinel lymph node biopsy (SLNB) has become the standard axilla staging procedure in patients with early stage breast

cancer due to its lower morbidity rate and similar accuracy compared to axillary lymph node dissection (ALND) [2]. However, SLNB requires preoperative lymphoscintigraphy and a detailed pathological examination. In addition, it is a time-consuming complicated process [3]. Although SLNB has high sensitivity and specificity values in detecting axillary metastatic lymph node in breast cancer patients [4], it has also been reported to give false negative results [5-7]. It is an invasive procedure with complications such as infection, lymphedema and seroma [8]. For these reasons,

it is important to evaluate the axillary lymph node metastasis status by non-invasive imaging methods before surgery in patients with breast cancer [9, 10].

In addition to detecting the presence of distant organ metastasis in patients with breast cancer, 2-deoxy-2-[fluorine-18] fluoro-D-glucose integrated with computed tomography (^{18}F FDG PET/CT), which shows the glucose metabolism of the tissue, provides valuable information in detecting axillary lymph node metastasis. High sensitivity and specificity values have been reported for the success of ^{18}F FDG PET/CT in detecting metastatic lymph nodes in the axilla in patients with breast cancer [9, 11, 12].

Another non-invasive imaging method, magnetic resonance imaging (MRI), which is applied with dynamic contrast enhancement (DCE) and the diffusion-weighted imaging (DWI) technique, is used to evaluate the presence of axilla lymph node metastasis in patients with breast cancer [13, 14]. High sensitivity and specificity values of MRI applied with these two techniques have been reported in detecting axillary metastatic lymph nodes in breast cancer patients [15-17].

In this study, we investigated the success of each and their combined use of ^{18}F FDG PET/CT and DCE/DWI-MRI in detecting axillary metastatic lymph nodes in patients with newly diagnosed breast cancer

Materials and methods

The Clinical Research Ethics Committee of our institute reviewed and approved this retrospective study (2019/136). As this was a retrospective study, it was exempt by the institutional review board from the need for informed consent. All procedures performed in studies involving human participants were in accordance with the Helsinki declaration.

Patient selection: We retrospectively reviewed the data of patients diagnosed with breast cancer between March 2017 and January 2019 and who underwent ^{18}F FDG PET/CT and MRI before treatment. We included 113 patients who underwent ^{18}F FDG PET/CT, 102 of these patients also had MRI. We did not include patients who received neoadjuvant therapy. All patients had undergone SLNB or ALND. We included patients with invasive ductal carcinoma.

Surgical method: SLNB was applied to 60 patients who were clinically and radiologically axillary lymph node metastasis free; ALND was applied to 79 patients. Axillary dissection was performed in 53 of these patients whose axilla was clinically and radiologically metastatic. In 9 of these patients, the frozen result was positive for metastasis, while the frozen result was suspicious in terms of metastasis in 3 of them. In 3 patients, ALND was performed due to the detection of suspicious lymph nodes intraoperatively and in 11 patients due to the absence of sentinel lymph nodes (N = 26).

Nuclear medicine method (lymphoscintigraphy) was not used for SLNB. After the injection of "isosulfan blue" into/around the tumour or around the nipple, the lymph nodes which were stained blue in the axilla were excised.

^{18}F -FDG PET/CT procedures: A PET/CT scanner Biograph mCT (Siemens Healthcare, Erlangen, Germany) was used. After at least 4 hours of fasting, patients with a blood glucose level of < 200 mg/dl were administered a FDG injection at an approximate dose of 3.7 MBq/kg. After median 61 minutes [min-max 52-81 minutes], imaging was performed in the supine position with arms up. The PET imaging was adjusted to 2 minutes per bed position. Low-dose CT parameters were as follows:

voltage, 120 kV, CARE Dose 4D mA tube current and slice thickness 5.00 mm.

¹⁸F-FDG PET/CT parameters: We evaluated the long diameter of the primary tumour (Tsize), the maximum standardised uptake value of the primary tumour normalised to body weight (SUVmaxT), the short diameter of the axillary lymph node (LnDPET/CT), the maximum standardised uptake value of the axillary lymph node normalised to body weight (SUVmaxLn), the metabolic tumour volume of the primary tumour according to the 40% threshold of the SUVmaxT (MTV) and the presence of multifocality of the primary tumour.

¹⁸F FDG PET/CT image analyses: The Siemens Healthineers Syngo.via VB30 workstation, MM Oncology, post-processing unit was used for analyses. All analyses were performed by a Nuclear Medicine Specialist (O.K.) with 9 years of PET/CT experience.

MRI procedure: Magnetic Resonance imaging was performed on a 3 Tesla MR (Discovery w750, GE Healthcare, United States) device with an 8-channel breast coil in the prone position. Following conventional images, diffusion-weighted images and pre-contrast images, dynamic images were obtained by intravenous injection of contrast material through the antecubital vein.

For all patients, T2-weighted (FSE-IDEAL) axial section (time to repetition (TR)/TE: 7127/85 ms; section thickness 3.5 mm; field of view (FOV) 400 mm), T1-weighted (FSE) axial section (TR/TE: 838 ms/12 ms; slice thickness 3.5 mm; FOV: 400 mm), STIR axial section (TR/TE: 7673 ms/32 ms; TI: 180 ms; slice thickness 3.5 mm; FOV: 400 mm) were obtained.

The DWI was obtained at two different b values (50 s/mm², 800 s/mm²) with the echo-planar SE T2 weighted sequence (TR/TE: 6193 ms/18 ms;

cross sectional area 4 mm; FOV: 400 mm) in the axial plane. For DCE, gadobutrol (Gadovist; Bayer Schering Pharma, Berlin, Germany) was administered intravenously at a dose of 0.1 mmol/kg with an automatic injector at a speed of 3 ml/sec, and high-resolution T1-weighted oil-suppressed TSE axial and sagittal section (TR/TE: 5 ms /2.3 ms; slice thickness 0.8 mm; FOV: 360 mm, flip angle: 10) images were obtained. The DCE sequence was performed by axial imaging obtained at 70, 130, 190, 250 and 310 seconds in pre-contrast and post-contrast dynamic series.

MRI parameters: We evaluated the short diameter of axillary lymph nodes and the presence of fatty hilum absence. The ADC values were measured.

MRI image analysis: The MRI images of the patients were evaluated without knowing the pathology results and PET/CT findings. All analyses were performed by a Radiologist (H.G.) with 8 years of MRI experience.

ADC measurement technique: Lymph nodes with contrast enhancement in DCE and higher signal intensity in DWI were detected in the axilla. We then manually drew ROIs from 3 sections with a standard area of 0.25-0.35 mm² on the relevant region on the ADC map and obtained the mean ADC values.

The median time between ¹⁸F FDG PET/CT and MRI was 3 days [min: 0, max: 10]. There was a median of 11 days (minimum: 2, maximum: 29) between MRI and axillary surgery and a median of 9 days (min: 3, max: 22) between ¹⁸F FDG PET/CT and axillary surgery.

Statistical analysis: Continuous demographic data were analysed according to normality tests. Parametric data were reported as mean ± standard deviation and non-parametric data as median (min-max). Differences between groups were analysed using Student's t-test in

parametric data and Mann-Whitney U tests in non-parametric data. Discontinuous variables were shown as frequency. We used receiver operating characteristic (ROC) curve analysis to evaluate the diagnostic performance of the methods and to determine the threshold value. Univariate and multivariate logistic regression analyses were used to determine the relationship of test parameters of the patients at risk for axillary lymph node metastasis. Statistical significance value was accepted as 0.05. The software package SPSS v. 25 (Chicago, USA) was used for statistical analysis.

Results

In total, 113 female patients (mean age: 55.6 standard deviation (SD): 13.36) who were diagnosed with breast cancer and underwent ^{18}F FDG PET/CT were evaluated. One hundred and two of these patients also had MRI. Of these, 97 patients were luminal, 6 patients were Her2-positive, and 10 patients were in the triple negative (TN) receptor subgroup. The presence of axillary lymph node metastasis was confirmed histopathologically in 58 patients. Axillary lymph node metastasis was not detected in 55 patients. Patient and tumour characteristics are given in Tables 1 and 2.

Visual analysis: We performed visual analysis in 102 patients who underwent both ^{18}F FDG PET/CT and MRI. Histopathological metastasis was detected in 52 of these patients; metastasis was not detected in 50 patients. The ^{18}F FDG PET/CT detected 41 (79%) of 52 patients with axillary lymph node metastasis and failed to detect axillary lymph node metastasis in 11 patients (21%). The mean value of the short diameter in the lymph nodes of 11 patients in whom ^{18}F FDG PET/CT could not detect axillary lymph node metastasis was 5.14 ± 0.9 mm [min: 4 mm, max: 7 mm].

Table 1. Mean-median values of parameters evaluated by MRI and ^{18}F FDG PET/CT.

| Parameters | Mean \pm SD | Median [Min-Max] |
|----------------------------|-----------------|------------------|
| ADC (mm ² /sec) | 1.18 \pm 0.27 | 1.21 (0.65-2.1) |
| LnDMRI (mm) | 9 \pm 5 | 8 (4-32) |
| LnDPET/CT (mm) | 8 \pm 5 | 7 (3-32) |
| LnSUVmax | 3.63 \pm 4.46 | 1.40 (0.50-19.3) |
| MTV (cm ³) | 6.07 \pm 7.63 | 3.70 (0.40-55) |
| SUVmaxT | 9.49 \pm 9.11 | 6.95 (1.30-73.5) |
| Tsize (mm) | 23 \pm 11 | 21 (8-60) |

ADC, apparent diffusion coefficient; MTV, metabolic tumour volume; LnDMRI, short diameter of the largest axillary lymph node measured by MRI; LnDPET/CT, short diameter of the largest axillary lymph node measured by PET/CT; LnSUVmax, SUVmax of the axillary lymph node; SUVmaxT, SUVmax of the primary tumour; Tsize, long diameter of the primary tumour.

Table 2. Tumour characteristics.

| Parameters | | N / % |
|---------------------|-----------------|-------|
| ALNM | No | 55/49 |
| | Yes | 58/51 |
| Multifocality | No | 83/73 |
| | Yes | 30/27 |
| Receptor Subtype | Luminal | 97/86 |
| | HER2+ | 6/5 |
| | Triple negative | 10/9 |
| Fatty Hilum Absence | No | 33/32 |
| | Yes | 69/68 |

ALNM, Axillary lymph node metastasis status

The ^{18}F FDG PET/CT was false positive in 3 of 50 patients (6%) without axilla lymph node metastasis. In 47 patients (94%), ^{18}F FDG PET/CT was able to detect no axillary lymph node metastasis. For the axillary lymph node short diameter > 6 mm, we found a 79% sensitivity of ^{18}F FDG PET/CT to detect the presence of metastasis, with a specificity of 70.9% (AUC = 0.821, $p < 0.001$) (Figure 1).

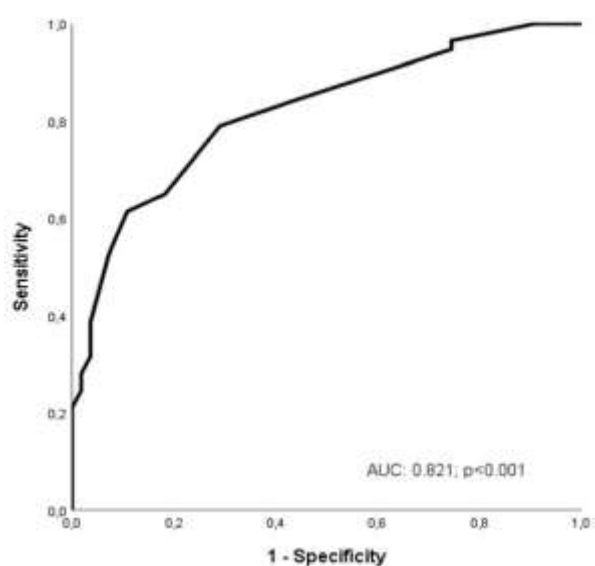


Figure 1. ROC curve showing the success of ^{18}F FDG PET/CT in detecting axillary metastatic lymph nodes when adopting a 6-mm threshold value for lymph node short diameter.

Magnetic resonance imaging (DCE + DWI) was performed in 102 patients and detected 30 (57.7%) of 52 patients with lymph node metastasis. The short-diameter mean value of lymph nodes of 22 patients in whom MRI could not detect lymph node metastasis was $7.1\text{mm} \pm 1.16$ [min: 5 mm, max: 9 mm]. The MRI detected 48 (96%) of 50 patients without axillary lymph node metastasis and was false positive in only 2 patients (4%).

When ^{18}F FDG PET/CT and MRI results were evaluated together ($n = 102$), ^{18}F FDG PET/CT + MRI detected 42 (81%) of 52 patients with

axillary lymph node metastasis, but could not detect 10 patients (19%). Short-diameter mean values of lymph nodes in these 10 patients were 5 ± 0.9 mm and 6.5 ± 0.85 mm for ^{18}F FDG PET/CT and MRI, respectively. The $\text{MR}^1 + ^{18}\text{F}$ FDG PET/CT detected 49 (98%) of 50 patients without axillary lymph node metastasis, with a false positive result in only 1 patient. The efficiency of the ROC curve of ^{18}F FDG PET/CT, MRI and $\text{MR}^1 + ^{18}\text{F}$ FDG PET/CT in detecting axillary metastatic lymph nodes is given in Figure 2. The sensitivity, specificity, accuracy, positive predictive values and negative predictive values of each of the ^{18}F FDG PET/CT, MRI, ^{18}F FDG PET/CT + MRI in detecting axillary metastatic lymph nodes are given in Table 3.

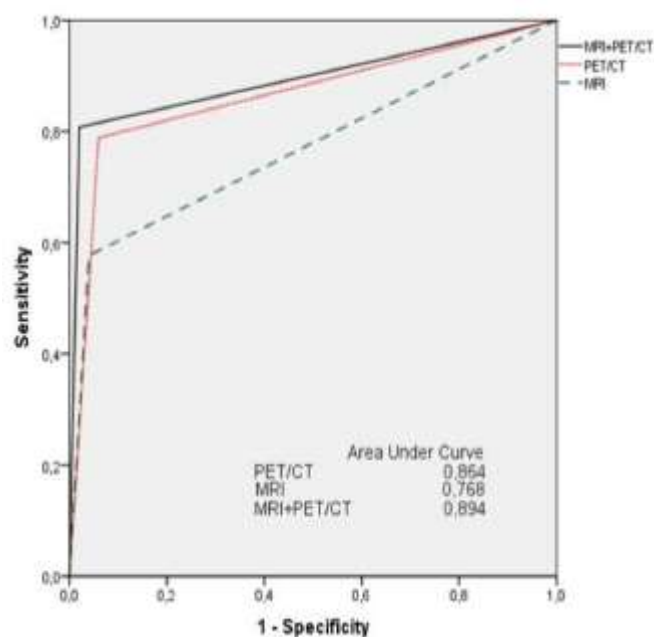


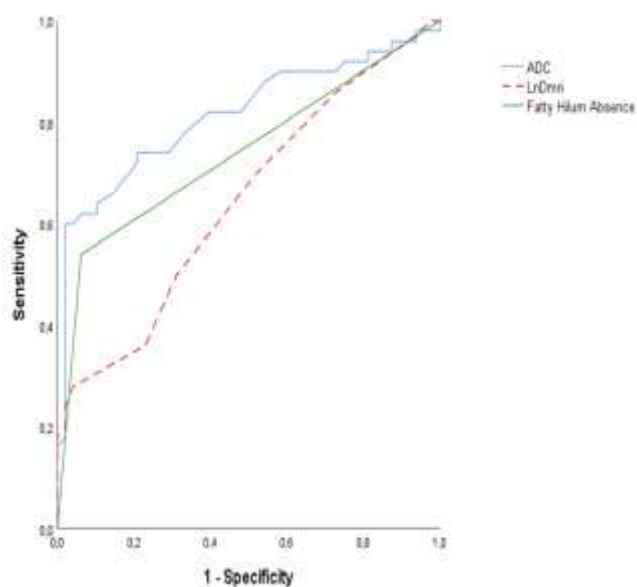
Figure 2. ROC curve demonstrating the success of ^{18}F FDG PET/CT, MRI and $\text{MR}^1 + ^{18}\text{F}$ FDG PET/CT in detecting axillary metastatic lymph nodes.

Quantitative analysis: We evaluated the MRI parameters [ADC, LnDMRI, fatty hilum absence] of 102 patients in univariate logistic regression analysis. In detecting lymph node metastasis, we performed ROC analysis and set

Table 3. Sensitivity, specificity, accuracy, positive predictive value, negative predictive values of ^{18}F FDG PET/CT, MRI and ^{18}F FDG PET/CT + MRI.

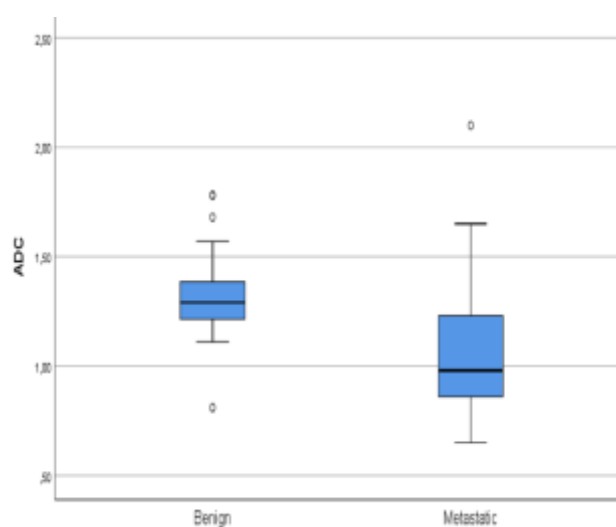
| Parameters | ^{18}F FDG PET/CT | MRI | ^{18}F FDG PET/CT + MRI |
|-------------------------------|----------------------------|------------------------|----------------------------------|
| Sensitivity (%) | 78.85 (65.3-88.94) | 70.27 (58.52-80.34) | 83.87 (72.33-91.98) |
| Specificity (%) | 94 (83.45-98.74) | 96.15 (86.79-99.53) | 98.04 (89.55-99.95) |
| Positive predictive value (%) | 93.18 (81.89-97.64) | 96.3 (86.89-99.03) | 98.11 (88.16-99.73) |
| Negative predictive value (%) | 81.03 (71.56-87.89) | 69.44 (61.46-76.41) | 83.33 (73.89-89.93) |
| Accuracy (%) | 86.27 (78.04-92.29) | 80.95 (73-87.4) | 90.27 (83.25-95.04) |

a threshold value of $1.2 \times 10^{-3} \text{ mm}^2/\text{sec}$ to obtain optimal sensitivity and specificity values for ADC. In univariate analysis, LnDMRI (Odds Ratio (OR) = 1.254, $p = 0.01$, 95% CI: 1.056-1.489), $\text{ADC} \leq 1.2 \times 10^{-3} \text{ mm}^2/\text{sec}$ (OR = 10.815, $p < 0.001$, 95% CI: 4.223-27.701) and lymph node fatty hilum absence (OR: 18, $p < 0.001$, 95% CI: 4.937-65.623) were statistically significant predictors for detecting axillary lymph node metastasis (Figure 3).

**Figure 3.** ROC curve demonstrating the success of MRI parameters in detecting axillary metastatic lymph nodes.

Multivariate logistic regression analysis showed that, $\text{ADC} \leq 1.2 \times 10^{-3} \text{ mm}^2/\text{sec}$ (OR = 4.472, $p = 0.008$, 95% CI: 1.484-13.479) and fatty hilum absence (OR = 6.703, $p = 0.011$, 95% CI: 1.537-29.228%) were independent predictors for detecting axillary lymph node metastasis.

We found a statistically significant difference between the mean ADC values of metastatic and benign lymph nodes (benign group mean ADC value: 1.31 ± 0.17 , metastatic group mean ADC value: 1.05 ± 0.27 , $p < 0.001$) (Figure 4).

**Figure 4.** Boxplot graph showing ADC values in metastatic and non-metastatic lymph nodes.

We evaluated the success of ^{18}F FDG PET/CT in detecting axillary lymph nodes in 113 patients with univariate logistic regression analysis. The parameters, Tsize (OR = 1.068, $p = 0.002$, 95CI 1.025-1.113%), MTV (OR = 1.082, $p = 0.034$, 95CI 1.006-1.163%), ^{18}F FDG PET/CT-multifocality (OR = 2.625, $p = 0.036$, 95CI 1.063-6.478%), LnDPET/CT (OR = 1.520, $p < 0.001$, 95CI%: 1.269-1.820), SUVmaxLn (OR = 2.213, $p < 0.001$, 95CI 1.533-3.193) were statistically significant predictors in detecting axillary metastatic lymph nodes, whereas SUVmaxT (OR = 1.011, $p = 0.608$, 95 CI 0.969-1.055) was not a reliable indicator in univariate analysis. We performed ROC analysis to obtain optimal sensitivity and specificity values of SUVmaxLn in detecting axillary lymph node metastasis and determined the threshold value 2 for SUVmaxLn. We created the model with the Backward LR method for multivariate logistic regression by including the parameters at $p < 0.2$ as a result of univariate analysis. In the multivariate logistic regression analysis, among the ^{18}F FDG PET/CT parameters, only SUVmaxLn > 2 (OR = 33.077, $p < 0.001$, 95CI%: 10.911-100.270) was an independent predictor in detecting axillary metastatic lymph nodes.

We included DCE-DWI MRI and ^{18}F FDG PET/CT parameters with $p < 0.2$ in the multivariate analysis as a result of univariate analysis. Multivariate logistic regression analysis showed that, $\text{ADC} \leq 1.2 \times 10^{-3} \text{ mm}^2/\text{sec}$ (OR = 6.665, $p = 0.001$, 95CI%: 2.181-20.370) and $\text{LnSUVmax} > 2$ (OR = 15.2, $p < 0.001$, 95CI%: 4.587-50.376) were independent predictors in detecting axillary metastatic lymph nodes. The sensitivity of SUVmaxLn > 2 was 73.7%, with a specificity of 92.7 (AUC = 0.845, $p < 0.001$). For $\text{ADC} \leq 1.212 \times 10^{-3} \text{ mm}^2/\text{sec}$, sensitivity was 74% and specificity was 79.2 (AUC: 0.814, $p < 0.001$) (Figure 5).

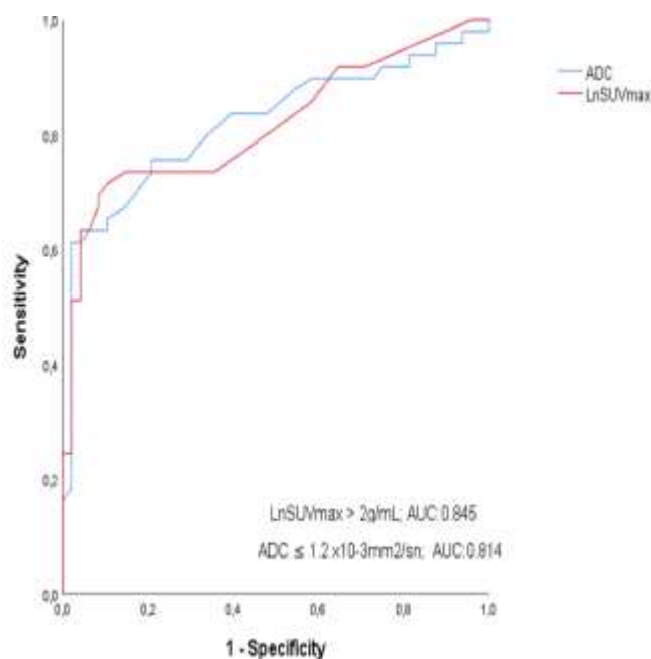


Figure 5. ROC curve showing success in detecting the presence of axillary lymph node metastasis for SUVmaxLn > 2 and $\text{ADC} \leq 1.2 \times 10^{-3} \text{ mm}^2/\text{sec}$.

We performed Cohen's kappa analysis between visual analysis results of ^{18}F FDG PET/CT and MRI. We observed a satisfactory value of agreement between the modalities (kappa: 0.669, $p < 0.001$). We also found a good agreement between the total result of MRI + ^{18}F FDG PET/CT visual evaluation and histopathological results (kappa: 0.785, $p < 0.001$).

Discussion

In this study, we visually and quantitatively evaluated the success of using ^{18}F FDG PET/CT, (DCE+DWI) MRI and a combination of them in detecting axillary lymph node metastasis in patients with newly diagnosed breast cancer.

In the visual analysis, we found a sensitivity of 78% and a specificity of 94% for ^{18}F FDG PET/CT; a sensitivity of 70% and a specificity of 96% for MRI. In the meta-analysis of 21 studies in 1,905 patients, the sensitivity of ^{18}F FDG PET/CT was 40 to 89% (pooled 64%),

with a specificity of 84 to 94% (pooled 93%). The sensitivity of MRI was 40 to 100% (pooled: 82%), with a specificity of 44 to 100% (pooled 94%) [18]. We observed an increase in sensitivity and specificity values when MRI and ^{18}F FDG PET/CT were used together (sensitivity: 83.8%, specificity: 98%). In another study in which 215 patients were evaluated, the total sensitivity of MRI and ^{18}F FDG PET/CT used together was 72.3, with a specificity of 92.4. Higher sensitivity and specificity values were obtained when used together than when used separately (sensitivity and specificity for MRI: 67.5 and 78%, for ^{18}F FDG PET/CT: 62.7 and 88.6%) [19].

Primary tumour MTV, Tsize, multifocality, LnDPET/CT, SUVmaxLn were statistically significant ^{18}F FDG PET/CT parameters for the presence of axillary lymph node metastasis in the univariate analysis. In the multivariate analysis, only SUVmaxLn was an independent parameter for the presence of axillary lymph node metastasis. In a study with 173 patients, only MTV was associated with the presence of axillary lymph node metastasis in T2 and T3 tumours, while MTV in T1 tumours was not associated with axillary lymph node metastasis [20]. In another study, only total lesion glycolysis (TLG) was an independent marker for the presence of axillary lymph node metastasis among primary tumour parameters [21]. In a study with 671 patients who were classified according to receptor subtypes as ER-positive/HER2-negative and HER2-positive, primary tumour SUVmax (> 4.25) and tumour size was associated with the presence of axillary lymph node metastasis. In patients of the triple negative (TN) receptor subgroup, primary tumour characteristics were not associated with the presence of axillary lymph node metastasis [22]. When we determined a threshold value of 2 for SUVmaxLn, we found

a sensitivity of 73.7%, and a specificity of 92.7%. In a study that included 196 patients, axillary lymph node SUVmax was associated with metastasis; when the authors took SUVmax threshold value as "1", they found a sensitivity of 53.8% and a specificity of 93.9% [23].

In this study, ADC values of metastatic axillary lymph nodes were lower than those of non-metastatic lymph nodes, similar to previous findings [16, 24]. For an ADC value of $1.2 \times 10^{-3} \text{ mm}^2/\text{sec}$, we found satisfactory values of sensitivity and specificity in detecting axillary lymph node metastasis. In a study involving 110 patients, the authors found a threshold value of $0.90 \times 10^{-3} \text{ mm}^2/\text{sec}$ for ADC, with a sensitivity of 100% and a specificity of 83.3%. We assumed that one of the reasons for this difference may be the fact that not all of the patients' imaging was performed with 3T MRI [24]. In another study performed with 3Tesla MRI in 52 patients, the sensitivity was 72.4% and the specificity was 79.6% for the ADC value of $0.812 \times 10^{-3} \text{ mm}^2/\text{sec}$. [25].

We found a significant relationship between the absence of fatty hilum in lymph nodes and the presence of axillary lymph node metastasis. In a study with 56 patients, the authors found a significant relationship between the absence of fatty hilum in lymph nodes and metastasis [26]. The main limitation of our study is that it is single-centred and retrospective. Although all our patients had IDC, we the patient group was not enough to analyse according to the hormone receptor status. We could not assess the cortical thickness parameter of the lymph nodes although it was an important criterion for axillary lymph node metastasis.

In conclusion, $\text{LnSUVmax} > 2$ and $\text{ADC} \leq 1.2 \times 10^{-3} \text{ mm}^2/\text{sec}$ were independent predictors in detecting axillary lymph node metastasis in patients with newly diagnosed breast cancer.

Funding: The author(s) received no financial support for the research, authorship, and/or publication of this article.

Conflict of Interest: The authors declare that they have no conflict of interest.

Ethical statement: The study was approved by the Local Ethics Committee of Recep Tayyip Erdogan University (Date and Decision no: 2019/136), and written informed consent was obtained from each subject.

Open Access Statement

This is an open access journal which means that all content is freely available without charge to the user or his/her institution under the terms of the Creative Commons Attribution Non-Commercial License (<http://creativecommons.org/licenses/by-nc/4.0>). Users are allowed to read, download, copy, distribute, print, search, or link to the full texts of the articles, without asking prior permission from the publisher or the author.

References

- [1]Carter CL, Allen C, Henson DE. Relation of tumor size, lymph node status, and survival in 24,740 breast cancer cases. *Cancer*. 1989; 63(19):181-87.
- [2]Crane-Okada R, Wascher RA, Elashoff D, et al. Long-term morbidity of sentinel node biopsy versus complete axillary dissection for unilateral breast cancer. *Ann Surg Oncol*. 2008; 15(7):1996-2005.
- [3]Purushotham AD, Upponi S, Klevesath MB, et al. Morbidity after sentinel lymph node biopsy in primary breast cancer: results from a randomized controlled trial. *J Clin Oncol*. 2005; 23(19):4312-21.
- [4]Veronesi U, Paganelli G, Viale G, et al. A randomized comparison of sentinel-node biopsy with routine axillary dissection in breast cancer. *N Engl J Med*. 2003; 349(6):546-53.
- [5]Monzawa S, Adachi S, Suzuki K, et al. Diagnostic performance of fluorodeoxyglucose-positron emission tomography/computed tomography of breast cancer in detecting axillary lymph node metastasis: comparison with ultrasonography and contrast-enhanced CT. *Ann Nucl Med*. 2009; 23(10):855-61.
- [6]McMasters KM, Tuttle TM, Carlson DJ, et al. Sentinel lymph node biopsy for breast cancer: a suitable alternative to routine axillary dissection in multi-institutional practice when optimal technique is used. *J Clin Oncol*. 2000; 18(13):2560-66.
- [7]Krag DN, Anderson SJ, Julian TB, et al. Technical outcomes of sentinel-lymph-node resection and conventional axillary-lymph-node dissection in patients with clinically node-negative breast cancer: results from the NSABP B-32 randomised phase III trial. *Lancet Oncol*. 2007; 8(10):881-88.
- [8]Wilke LG, McCall LM, Posther KE et al. Surgical complications associated with sentinel lymph node biopsy: results from a prospective international cooperative group trial. *Ann Surg Oncol*. 2006; 13(4):491-500.
- [9]Heusner TA, Kuemmel S, Hahn S, et al. Diagnostic value of full-dose FDG PET/CT for axillary lymph node staging in breast cancer patients. *Eur J Nucl Med Mol Imaging*. 2009; 36(10):1543-50.
- [10]Kvistad K, Rydland J, Smethurst H-B, et al. Axillary lymph node metastases in breast cancer: preoperative detection with dynamic contrast-enhanced MRI. *Eur Radiol*. 2000; 10(9):1464-71.
- [11]Ahn J-H, Son EJ, Kim J-A, et al. The role of ultrasonography and FDG-PET in axillary lymph node staging of breast cancer. *Acta Radiol*. 2010; 51(8):859-65.

- [12] Peare R, Staff RT, Heys SD. The use of FDG-PET in assessing axillary lymph node status in breast cancer: a systematic review and meta-analysis of the literature. *Breast Cancer Res Treat.* 2010; 123(1):281-90.
- [13] Zhang Y, Qin Q, Li B, et al. Magnetic resonance imaging for N staging in non-small cell lung cancer: A systematic review and meta-analysis. *Thorac Cancer.* 2015; 6(2):123-32.
- [14] Plana MN, Carreira C, Muriel A, et al. Magnetic resonance imaging in the preoperative assessment of patients with primary breast cancer: systematic review of diagnostic accuracy and meta-analysis. *Eur Radiol.* 2012; 22(1):26-38.
- [15] Kim EJ, Kim SH, Kang BJ, et al. Diagnostic value of breast MRI for predicting metastatic axillary lymph nodes in breast cancer patients: diffusion-weighted MRI and conventional MRI. *J Magn Reson Imaging.* 2014; 32(10):1230-36.
- [16] Fornasa F, Nesoti MV, Bovo C, et al. Diffusion-weighted magnetic resonance imaging in the characterization of axillary lymph nodes in patients with breast cancer. *J Magn Reson Imaging.* 2012; 36(4):858-64.
- [17] Kamitani T, Hatakenaka M, Yabuuchi H, et al. Detection of axillary node metastasis using diffusion-weighted MRI in breast cancer. *Clin. Imaging.* 2013; 37(1):56-61.
- [18] Liang X, Yu J, Wen B, et al. MRI and FDG-PET/CT based assessment of axillary lymph node metastasis in early breast cancer: a meta-analysis. *Clin Radiol.* 2017; 72(4):295-301.
- [19] An Y-S, Lee D, Yoon J-K, et al. Diagnostic performance of 18F-FDG PET/CT, ultrasonography and MRI. *Nuklearmedizin.* 2014; 53(3):89-94.
- [20] An Y-S, Kang DK, Jung Y, et al. Volume-based metabolic parameter of breast cancer on preoperative 18F-FDG PET/CT could predict axillary lymph node metastasis. *Medicine.* 2017; 96(45):e8557.
- [21] Yoo J, Kim BS, Yoon H-J. Predictive value of primary tumor parameters using 18 F-FDG PET/CT for occult lymph node metastasis in breast cancer with clinically negative axillary lymph node. *Ann Nucl Med.* 2018; 32(9):642-48.
- [22] Kim JY, Lee SH, Kim S, et al. Tumour 18 F-FDG uptake on preoperative PET/CT may predict axillary lymph node metastasis in ER-positive/HER2-negative and HER2-positive breast cancer subtypes. *Eur Radiol.* 2015 ;25(4):1172-81.
- [23] Sun WY, Choi YJ, Song Y-J. Prediction of Axillary Nodal Status according to the Axillary Lymph Node to Primary Breast Tumor Maximum Standardized Uptake Value Ratio on 18 F-fluorodeoxyglucose Positron Emission Tomography/Computed Tomography. *J Breast Dis.* 2016; 4(2):92-99.
- [24] Chung J, Youk JH, Kim J-A, et al. Role of diffusion-weighted MRI: predicting axillary lymph node metastases in breast cancer. *Acta Radiol.* 2014; 55(8):909-16.
- [25] Rautiainen S, Könönen M, Sironen R, et al. Preoperative axillary staging with 3.0-T breast MRI: clinical value of diffusion imaging and apparent diffusion coefficient. *PLoS One.* 2015; 10:e0122516.
- [26] Mortellaro VE, Marshall J, Singer L, et al. Magnetic resonance imaging for axillary staging in patients with breast cancer. *J Magn Reson Imaging.* 2009; 30(2):309-12.